

Nanoscale

Accepted Manuscript



This is an *Accepted Manuscript*, which has been through the Royal Society of Chemistry peer review process and has been accepted for publication.

Accepted Manuscripts are published online shortly after acceptance, before technical editing, formatting and proof reading. Using this free service, authors can make their results available to the community, in citable form, before we publish the edited article. We will replace this *Accepted Manuscript* with the edited and formatted *Advance Article* as soon as it is available.

You can find more information about *Accepted Manuscripts* in the [Information for Authors](#).

Please note that technical editing may introduce minor changes to the text and/or graphics, which may alter content. The journal's standard [Terms & Conditions](#) and the [Ethical guidelines](#) still apply. In no event shall the Royal Society of Chemistry be held responsible for any errors or omissions in this *Accepted Manuscript* or any consequences arising from the use of any information it contains.

ARTICLE

Synthesis of Ordered Mesoporous Crystalline CuS and Ag₂S Materials *via* Cation Exchange Reaction

Cite this: DOI: 10.1039/x0xx00000x

Jun Wang,^a Weiming Xu,^{*a} Haifeng Bao^b and Yifeng Shi^{*a,c}Received 00th January 2014,
Accepted 00th January 2014

DOI: 10.1039/x0xx00000x

www.rsc.org/

Cation exchange reaction is a strong tool for the synthesis of new ionic nanomaterials. Most of them are isolated nanoparticles with simple geometry feature, such as nanodots, nanorods and nanospheres. In this work, we demonstrated that ordered mesoporous CdS with a complex cubic *Ia3d* gyroid 3D bicontinuous porous structure and large particle size can be successfully converted to crystalline CuS and Ag₂S materials *via* cation exchange reaction without destroying the well-defined nanostructure. The crystal structure change is an important factor for a successful conversion when the reaction is carried out without the presence of silica template. In addition, the cation exchange reaction is sufficiently enough for a completely composition conversion even when the mesostructured CdS precursor is embedded inside a mesoporous silica matrix. Our results indicate that cation exchange reaction may be applied to highly complex nanostructures with extremely larger particle sizes.

Introduction

Materials with all kinds of specific nanostructures are highly desired in various research areas because of their size- and shape-tunable properties. Recently, pseudomorphic transformation became an efficient strategy for making new nanomaterials, in which the composition of a precursor material is converted to an aimed material while the nanostructure characteristics are well maintained.¹⁻⁶ Among them, cation exchange reaction is particularly a strong tool for the synthesis of metal chalcogenide semiconductors, which can occur completely and reversibly at room temperature with unusually fast reaction rates.⁵⁻⁸ However, in most of the successful cases, only isolated particles with simple geometry features, such as nanodots, nanorods and nanostars, were investigated.⁵⁻¹⁰ Only few of them involved more complicated nanostructures such as nanoparticles supported within a matrix material made of surfactant micelles array.¹¹ It was suspected that the volume change and the crystal phase transformation may bring insoluble issues for the more complex 3D nanostructures in cation exchange reaction. However, it has never been carefully investigated, which partially due to the lack of suitable precursor.

In the past two decades, ordered mesoporous materials have attracted lots of interests because of their unique structure characteristics and promising potentials in diverse applications.^{4, 12} Among them, ordered mesoporous metal chalcogenides are especially interesting as they combined the unique periodic porous structure with the semiconductor frameworks.^{4, 13, 14} The uniform nanosized frameworks bring all kinds of nano-effects, while the highly accessible inter-porous surface makes them feasible for interface related applications, such as sensing and photocatalysis. In

addition, the large particle size shows advantages in handling and processing comparing to the corresponding isolated nanoparticles.

Ordered mesoporous CdS, In₂S₃, ZnS, WS₂ and MoS₂ materials have been successfully synthesized by nanocasting method using mesoporous silica as hard template.^{4, 14, 15} However, it's hard to analogously synthesize other metal sulfides due to the lack of proper precursors or other tricky problems. Very recently, Jiao's group utilized mesostructured metal oxides (Fe₂O₃, Co₃O₄ and NiO) as precursor to synthesize mesoporous metal sulfides *via* H₂S/sulfur vapor treatment.¹⁶ The mesostructured metal oxides were prepared inside the mesoporous silica template *via* nanocasting method before the oxide-to-sulfide conversion. However, only few metal oxides can form ordered mesostructure inside the silica template to be used as the precursor for such a chemical transformation process, e. g. CuO is not one of them.

Among the currently available mesoporous crystalline metal chalcogenides, CdS is a strong ionic solid comparing to others, making it a perfect model precursor for cation exchange reaction. In this work, mesoporous crystalline CdS is utilized as a precursor to synthesize ordered mesoporous Ag₂S and CuS materials *via* cation exchange reaction. Both of them have never been reported by any other method. In order to investigate the cation exchange reaction in an complex nanostructure, mesoporous silica KIT-6 with 3D *Ia3d* gyroid pore structure was utilized as the hard template, which is one of the most complex well-defined nanostructures those we can make in lab. In addition, the highly ordered periodic structure make us can use X-ray diffraction techniques to precisely investigate the structure shrinkage/expansion rate during the cation exchange reaction, which can hardly be achieved in isolated nanoparticle systems.

Experimental

Synthesis of mesoporous silica template KIT-6:¹⁷

12 g of Pluronic P123 triblock copolymer, 20 mL of HCl (35 wt%) and 12 g of butanol were dissolved in 483 mL of water at 35°C. Then 25.8 g of tetraethyl orthosilicate (TEOS) were poured into the mixture and it was kept under stirring at 35°C for another 24 h. The mixture was then transferred into a hydrothermal bomb for hydrothermal treatment at 100°C for 48 h. The as-made KIT-6 was filtered, washed with ethanol and dried at room temperature in air. The P123 surfactant was subsequently removed by calcining in air at 550°C for 6 h to produce the mesoporous silica KIT-6 template.

Synthesis of CdS@KIT-6 intermediate and mesoporous CdS:¹⁸

5.2 g of Cd(NO₃)₂·4H₂O and 1.5 g of thiourea were dissolved in 30 mL of ethanol at room temperature. 2.7 g of KIT-6 template was added into the mixture under stirring. After the ethanol was evaporated up, the solid mixture was spread in five petri dishes (diameter: ~20 cm). The mixture was then heated in air inside an oven at 160°C for 24 h, leading to the formation of CdS@KIT-6 intermediate. The silica template can be removed by using 100 mL 2M NaOH aqueous solution as etching agent to get mesoporous CdS.

Cation exchange procedure for mesoporous Ag₂S:

2 g of AgNO₃ was dissolved in a mixture of 80 mL ethanol and 20 mL glycerol. Then 0.2 g of CdS@KIT-6 intermediate or 0.1 g of mesoporous CdS without the silica template was added into the solution for cation exchange reaction. The mixture was kept stirring for 10 h at room temperature. This process was repeated for one more cycle to ensure a complete cation exchange. The black product was filtered, washed and dried. In order to avoid the decomposition of AgNO₃, the entire process is carried out in the darkness.

Cation exchange procedure for mesoporous CuS:

6.6 g of Cu(NO₃)₂·3H₂O was dissolved in a mixture of 80 mL ethanol and 20 mL glycerol. 0.5 mL of HNO₃ (67 wt%) aqueous solution was added into the above solution to keep Cu²⁺ stable from forming Cu(OH)₂ precipitation. 0.5 g of CdS@KIT-6 intermediate or mesoporous CdS without the silica template was added in to the solution. The mixture was kept under stirring for 10 h at room temperature for cation exchange reaction. This process was repeated for one more cycle to ensure a complete cation exchange.

Characterization

Powder X-ray diffraction patterns were recorded with nickel-filtered Cu K α radiation ($\lambda = 1.5406 \text{ \AA}$) source on a Bruker D8 advance diffractometer (40 kV, 40 mA). Scanning electron microscope (SEM) images were obtained on S4800/FEI-quant-200F. Transmission electron microscope (TEM) images were collected on FEI-G2. Energy-dispersive X-ray spectroscopy (EDS) was taken on a FEI-G2 Transmission electron microscope.

Brunauer-Emmett-Teller (BET) surface area data was taken from Quadrasorb SI at 77 K and the pore size distribution was calculated from adsorption isotherm using Barrett-Jonyer-Halenda (BJH) method. The Raman data was recorded from Bruker Senterra, and the wave length of the exciting source is 532 nm.

Results and discussion

Mesoporous silica KIT-6 template was synthesized according the literature reports, which has a high symmetric gyroid bicontinuous 3D porous structure with *Ia3d* space group (Figure 1a).¹⁷ The hydrothermal treatment temperature is 100°C and the calcination temperature is 550°C in this work. The small-angle X-ray diffraction (XRD) pattern of the KIT-6 template shows more than 6 clear diffraction peaks (Figure S1), indicating that it has a highly ordered mesostructure. The corresponding cell parameter is estimated to be 23.5 nm. Nitrogen sorption analysis (Figure S2) found that the mean pore size and pore volume of the template is 8.5 nm and 1.15 cm³/g, respectively. All these values are very similar to those reported in literature.¹⁷

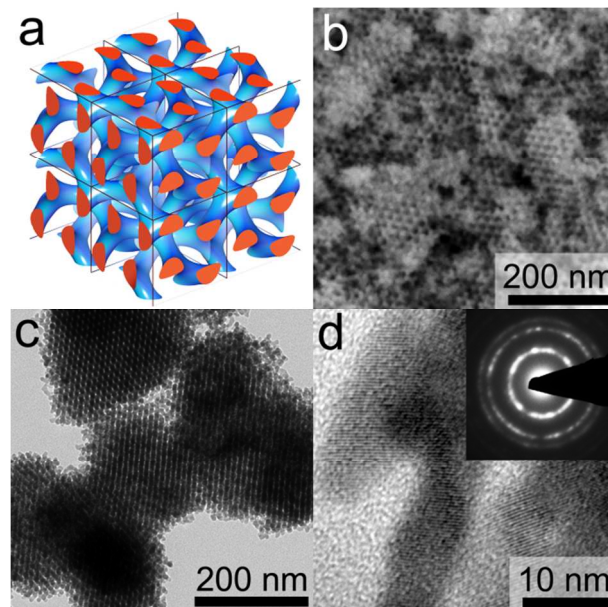


Fig. 1 (a) Structure model, (b) SEM, (c) TEM, (d) HRTEM images and SAED pattern of the mesoporous CdS material without the mesoporous silica template.

In the first step, a mesostructured crystalline CdS material was synthesized by using KIT-6 as a hard template *via* nanocasting method.¹⁸ Cd(NO₃)₂·4H₂O and thiourea, as metal and sulfur sources, were dissolved in ethanol and impregnated into the KIT-6 template. Nanostructured crystalline CdS was formed inside the KIT-6 template by heating the intermediate at 160°C in a common oven. XRD analysis reveals that the obtained CdS possesses a crystalline nature and all its XRD diffraction peaks can be indexed to the cubic phase CdS (Figure 2), in agree with the results reported in the literature reports.^{18, 19} The diffraction peaks at 26.4, 30.6, 43.8 and 54.4° corresponding to the (111), (200), (220), (222) lattice plates of

the cubic zinc blended crystal structure as shown in literature (JCPDS: 65-2887), respectively. The crystal grain size is estimated to be around 9.4 nm according to the Scherrer formula, which is quite close to the pore diameter of the KIT-6 template. It can be explained by that all the CdS particles are growth inside the mesopore of the KIT-6 template.

If the mesoporous silica template was removed by NaOH etching, an ordered mesoporous crystalline CdS can be obtained.¹⁸ Its small angle XRD pattern show a clear intensive diffraction peak and a weak broad peak at 2 theta value around 0.91° and 1.8° (Figure S3), respectively, indicating it successfully copied the highly ordered mesostructure from its mother template KIT-6. The SEM and TEM images (Figure 1b and c) directly show the ordered mesostructure of the mesoporous CdS sample. The sizes of the mesoporous CdS particles are generally larger than 200 nm, and some of them can even larger than 1 μm (Figure S4). HRTEM image and SAED patterns confirm that the framework of the mesoporous CdS is composed by cubic phase CdS nanocrystallites (Figure 1d). Nitrogen sorption analysis reveals it has a specific surface area of 133 m²/g, and a pore volume of 0.28 cm³/g, respectively. The mean pore size estimated by BJH method is approximately 4 nm (Figure S5), which is consistent with the wall thickness of KIT-6. All these result indicates that the Cd(NO₃)₂·4H₂O and thiourea were successfully converted into crystalline CdS with ordered mesostructure inside the KIT-6 template after the 160° C treatment.¹⁸

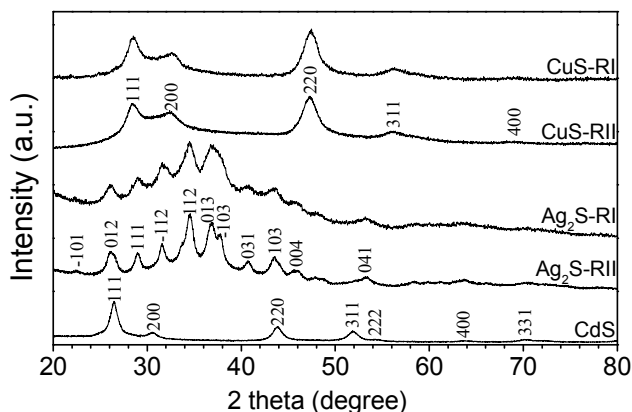


Fig. 2 Wide angle XRD patterns of the mesoporous CdS precursor, mesoporous Ag₂S and mesoporous CuS products synthesized *via* Route I (denoted as MS-RI) and Route II (denoted as MS-RII).

In ordered to convert the mesostructured CdS to other target mesoporous metal sulfide products *via* cation exchange reaction, two synthesis routes can be taken as shown in Figure 3. In Route I, mesoporous silica template is firstly removed by NaOH etching and the obtained mesoporous CdS is used as the direct precursor for cation exchange reaction. In this case, the entire surface of mesoporous CdS is accessible for cation exchange. Therefore, the diffusion length of cation ions is less than 10 nm, which is expected to be an advantage for a completely cation exchange. In route II, the CdS@KIT-6 intermediate was directly used for cation exchange before the silica template was removed. In this case, the

mesostructure is supposed to be more stable because the target products can only growth inside the mesopore space of the hard template. However, since the CdS precursor is confined inside the pore space of the silica template, only the limited outer surface is accessible for the aimed cations in this case. As a consequence, the diffusion length of cations has to be much longer, even longer than 1 μm, which may affect the reaction kinetics.

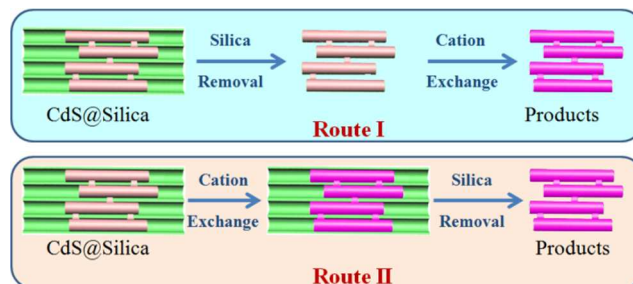


Fig. 3 Two synthesis route for the synthesis of mesoporous metal chalcogenides from mesostructured CdS precursor *via* cation exchange reaction.

In this work, AgNO₃ and Cu(NO₃)₂·4H₂O were used as Ag⁺ and Cu²⁺ sources, respectively. The solvent was made of ethanol and glycerol with 8:2 volume ratio. The CdS precursor, mesoporous CdS (in Route I) or mesostructured CdS@KIT-6 (in Route II), was added into the solution and kept stirring overnight for a completely cation exchange. Upon the cation exchange treatment, the colour of the sample powder tuned from orange to dark black immediately, suggesting a fast composition change is occurring. The cation exchange process was repeated for two cycles to insure a complete exchange of cations in all syntheses.

XRD analyses reveal that all of the mesoporous Ag₂S and CuS products collected after the cation exchange treatment show completely different diffraction patterns from that of their precursor CdS (Figure 2), indicating that a composition conversion of their crystalline frameworks occurred. In cases of Ag₂S, the XRD patterns of mesoporous Ag₂S synthesized from Route I is well consistent with the standard pattern of acanthite phase Ag₂S (JCPDS: 14-0072), which indicates that the CdS precursor has been successfully transform into crystalline Ag₂S *via* cation exchange reaction. As for CuS, the mesoporous CuS products synthesized *via* Route I possesses a cubic phase crystal structure without any noticeable impurity. In addition, the XRD pattern of mesoporous Ag₂S and mesoporous CuS products synthesized *via* Route II show very similar patterns with those synthesized *via* Route I, indicating that the presence of silica template did not affect the phase purity of the products. The CdS nanomaterials used for cation exchange in previous literature reports are all hexagonal wurtzite phase CdS material, which is a more stable crystal phase for CdS. Our results indicate that the cubic phase CdS nanomaterial can also be used as a precursor for cation exchange.

TEM observation reveals that the Ag₂S material synthesized *via* Route I still possess some mesoscale structure but without any long range ordering (Figure 4a). It seems that the Ag₂S grew inside the

mesopore and thus destroyed the ordering of the mesostructure. However, the whole particle size is still similar with its CdS precursor. Its small angle XRD pattern (Figure S3) do not show any noticeable diffraction peaks. It suggests that a local rearrangement occurred during the cation exchange process. Nitrogen sorption analysis also found that the pore volume and the specific surface area of this sample are decreased to only $0.06 \text{ cm}^3/\text{g}$ and $15 \text{ m}^2/\text{g}$, respectively. All these results confirm that the mesostructure is collapsed during the conversion from CdS to Ag_2S without the support of mesoporous silica template. In another hand, small angle XRD analysis (Figure S3) and TEM observation (Figure 4d) clearly reveals that mesoporous CuS products synthesized *via* Route I clearly possessed an ordered mesoporous structures. Nitrogen sorption analysis also found the mesoporosity is well preserved, and the specific surface area and pore volume are $106 \text{ m}^2/\text{g}$ and $0.29 \text{ cm}^3/\text{g}$. The above results show that mesoporous CdS without silica template can be successfully converted to ordered mesoporous CuS but failed in the conversion to Ag_2S .

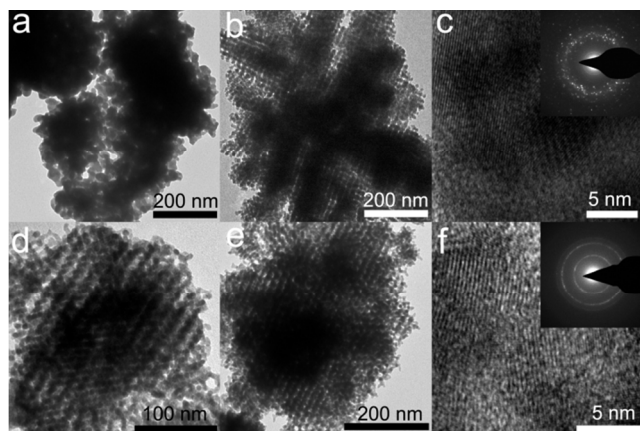


Fig. 4 TEM, HRTEM images and SAED patterns of mesoporous (a, b, c) Ag_2S and (d, e, f) CuS synthesized by (a, d) Route I or (b, c, e, f) Route II.

It has been reported that the volume change ratio is a key factor for ordered mesoporous structure in pseudomorphic transformation as in the second step of Route I.⁴ For example, the volume change values of the composition conversions from $\alpha\text{-Fe}_2\text{O}_3$ to Fe_3O_4 , Fe_3O_4 to $\gamma\text{-Fe}_2\text{O}_3$, Mn_2O_3 to Mn_3O_4 , Co_3O_4 to CoO , and Co_3O_4 to CoN , are +2.2%, +10.3%, +10.5%, -11.4% and -9.7%, respectively. In all of these cases, the ordered mesostructure was well preserved after the framework composition was converted from the former to the later ones by solid-gas reactions without the support of silica template.²⁰ Literature reports also showed that if the volume change ratio is higher than 50%, which equals to a 21% shrinkage in mesostructure cell parameter, the ordered mesostructure collapses after the conversion.²¹

In this work, as mentioned above, an ordered mesoporous CuS was successfully synthesized but the mesostructure of the obtained Ag_2S was collapsed (Figure 4a and d). The conversion from CdS to Ag_2S is accompanied by a 14.4% volume expansion in theory, which is higher than those in previously reported successful samples in

pseudomorphic transformation of ordered mesoporous structures. This may partially explain the mesostructure collapse of the Ag_2S product. However, the conversion from CdS to CuS is accompanied by a 20.3% shrinkage in volume and a 7.3% shrinkage in mesostructure cell parameter in theory, which is a much higher volume change ratio than all reported values. Interestingly, the mesostructure ordering is well maintained after the cation exchange in this case, as shown in Figure 4d. This result indicates that the volume change ratio is not the only key factor for the successful pseudomorphic transformation of ordered mesoporous materials.

We believe that the crystal structure change is another important factor. The obtained CuS possess a same cubic phase crystal structure with CdS. Therefore, the arrangement of S atoms keeps unchanged when Cd^{2+} was replaced by Cu^{2+} due to the thermodynamic driving force, except a shrinkage in cell parameter ($\sim 7.3\%$). While, in case of Ag_2S , the obtained product is in the form of acanthite phase with a monoclinic symmetry, which is the only stable form for Ag_2S at room temperature. The cubic phase Ag_2S , argentite phase, can only exist at temperatures above 173°C . This property means the S atoms have to be rearranged when CdS was converted to Ag_2S ,¹⁰ and we believe this rearrangement affected the mesostructure ordering in the cation exchange process. It has been reported that when a ultra-small CdSe nanomaterial with hexagonal crystal phase was converted to Ag_2Se with orthorhombic crystal phase *via* the cation exchange reaction, the particle shape is converted from nanorod to nanosphere.⁶ This rearrangement of S atoms, which leads to the shape change, is believed to be caused by the nonequilibrium state during the exchange, which brings significant structural distortions when the anions also have to be rearranged to achieve thermodynamically preferred crystal structure for the new composition.⁸ We believe the same crystal phase of CuS and CdS helps the mesoporous CuS to maintain the ordered mesoporous structure during the cation exchange reaction.

The composition conversions during the cation exchange reactions inevitably bring shrinkage or expansion in their crystal cell parameters, and therefore it will change the size of the products. However, in most literature reported cases, the precursors and the products are isolated nanocrystals with size less than 10 nm. The change of size parameters are generally less than 1 nm. It's hard to precisely investigate the size change value due to the lack of appropriated technology for isolated nanoparticles with ultra-small sizes, as well as the size distributions issues. The precursor used in this work, mesoporous CdS material, is composed by a complex but periodic 3D structure as shown in Figure 1a. The diameter of the building blocks of this structure is less than 10 nm. However, the building blocks are patterned with long range ordering. The periodic structure make us can record the structure shrinkage or expansion ratio by X-ray diffraction patterns (Figure S3). The cell parameters of CdS precursor and CuS product, estimated from the small angle XRD patterns, are 23.7 and 21.8 nm, respectively. The shrinkage ratio is calculated to be 8.0 %, which is very close to the shrinkage ratio (7.2%) in crystal cell parameter from CdS (0.583 nm) to CuS (0.541 nm), estimated from their wide-angle XRD patterns (Figure 2). This result indicates that the mesostructure is uniformly

shrinkage along with the shrinkage of crystal structure during the cation exchange reaction. And it suggest that the S atoms do not rearranged but just keep their structure and slightly shrinkaged upon the cation exchange between Cd^{2+} and Cu^{2+} .

In case of Route II, TEM observation reveals that both of the mesoporous Ag_2S and CuS products clearly possess ordered mesoporous structure as the silica template was removed after the cation exchange reaction, as shown in Figure 4b and e. For Ag_2S , the crystal phase is changed from cubic structure to monoclinic structure as same as that in Route I (Figure 2). But the ordered mesostructure is preserved in this case, which was also confirmed by its small angle XRD pattern (Figure S9). It can be explained by that the occurred rearrangement has to be confined inside the ordered pore space of KIT-6 template, because the silica template is made of covalent network and thus very stable in this case. Therefore, the mesostructure still maintained its structure regularity. Nitrogen sorption analyses revealed that both of them possess clear mesoporosity. The pore volume and specific surface area of mesoporous Ag_2S is calculated to be $0.10 \text{ cm}^3/\text{g}$ and $33 \text{ m}^2/\text{g}$, which are much smaller than those of mesoporous CdS . This can be explained by the large molecular weight and higher density of Ag_2S , comparing to CdS .

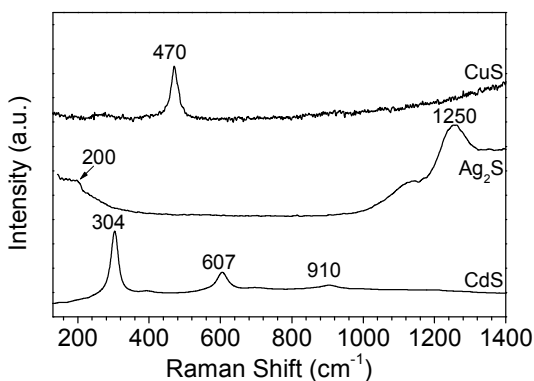


Fig. 5 Raman spectra of ordered mesoporous CdS precursor, Ag_2S and CuS products synthesized *via* Route II.

The clear crystal lattice fringes in its HRTEM image revealing the crystalline nature of the mesoporous Ag_2S product (Figure 4c). The interplanar crystal spacing is approximately 0.23 nm, corresponding to the (013) lattice planes of mesoporous Ag_2S . In addition, the selected-area electron diffraction (SAED) pattern (Fig 4c inset) also proves that the product is composed by Ag_2S nanocrystallites. The average crystal grain size is calculated to be 8.9 nm based on the d_{220} crystal lattice of Ag_2S at 34.7° from its XRD pattern. This value is quite close to the grain size of its precursor CdS (9.4 nm), indicating that the cation exchange process do not decrease the crystallinity of the framework. Interestingly, the crystallinity of Ag_2S synthesized *via* Route II is slightly higher than that of Ag_2S synthesized *via* Route I as shown in their wide angle XRD patterns (Figure 2). This can be explained by that the silica matrix slow down the conversion process due to the kinetic issues, and thus provide more time for the

crystal rearrangement during the cation exchange. The cation exchange process is too fast for the crystal structure rearrangement in Route I and therefore leads to a slightly lower crystallinity.

Similarly, small-angle XRD pattern (Figure S9) and TEM image (Figure 4e) both clearly reveals that mesoporous CuS synthesized *via* Route II possesses ordered mesoporous structures. HRTEM images (Figure 4f), SAED pattern (Figure 4f inset), and the XRD pattern (Figure 2) all confirm that the obtained mesoporous CuS possess a crystalline framework with similar crystallization degree with its CdS precursor. That is to say, mesoporous CdS can also be successfully converted to ordered mesoporous CuS *via* Route II.

It has been worried about that the present of silica template may affect the complete exchange of cations due to the kinetic issues. Therefore, the mesoporous Ag_2S and CuS products synthesized *via* Route II were carefully investigated by Raman spectra analysis (Figure 5). The Raman spectrum of mesoporous CdS consist of a fundamental band at approximately 304 cm^{-1} and its overtones, 607 and 910 cm^{-1} , as reported in literatures for bulk CdS and other CdS nanomaterials.²² After the Cd^{2+} were replaced by Ag^+ or Cu^{2+} *via* cation exchange reaction, the Raman spectra of the obtained products were clearly different from that of CdS . The Raman spectrum of mesoporous CuS product shows one strong and sharp band at 470 cm^{-1} , which was originates from the lattice vibration of the cubic phase CuS crystal.²³ The sharp peak reveals that the CuS is well crystallized, which is consistent with its XRD results (Figure 2). As for mesoporous Ag_2S , only weak bands those related to symmetric stretching mode are expected, because the Ag_2S unite is triatomic and non-linear. The broad band at $130 - 200 \text{ cm}^{-1}$ is coming from the Ag lattice vibrational modes.²⁴ The broad bands at 1250 cm^{-1} is assigned to the photo-decomposition products caused by laser beam during the measurement.²⁴ As shown in Figure 5, no signals from CdS is recorded in the Raman spectra of mesoporous Ag_2S and CuS products synthesized *via* Route II, which confirms that the chemical composition is transformed from CdS to CuS and Ag_2S after the cation exchange reaction despite of the presence of the silica matrix.

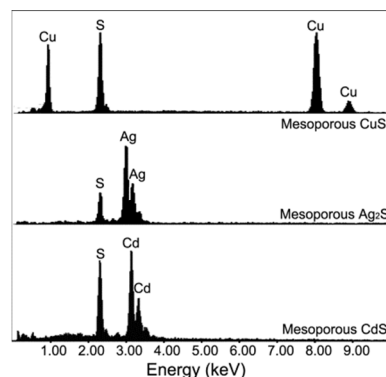


Fig. 6 EDS spectra of ordered mesoporous CdS precursor, Ag_2S and CuS products synthesized *via* Route II.

Energy Dispersive X-Ray Spectroscopy (EDS) analysis is also used to confirm the efficiency of cation exchange in this case (Fig. 6). The

absence of Cd²⁺ in both of the mesoporous Ag₂S and CuS products confirms that the Cd²⁺ ions were completely replaced by Ag⁺ and Cu²⁺ ions. The Ag:S and Cu:S ratios of the products are estimated to be 1.96 and 1.20. The lack of sulphur in mesoporous CuS product may attribute to the partially oxidation of sulphur by nitric acid, which was added into the solution to keep Cu²⁺ stable from forming precipitation.

In general, cation exchange is utilized for the synthesis of isolated nanoparticles, and therefore the diffusion lengths of the cations in those cases are generally less than 20 nm.⁵ In our synthesis, we took the CdS@KIT-6 intermediate as precursor Route II. The CdS crystal was confined inside the mesoporous silica and surrounded by the silica matrix, which means only limited outer surface of CdS was accessible for Ag⁺ and Cu²⁺ during the cation exchange process. The Cd²⁺ ions in the inner core also have to diffuse hundreds of nanometer distance before it entered into the solvent. While, XRD, Raman and EDS analyses all proved that CdS frameworks were entirely transformed to Ag₂S and CuS, respectively, indicating the presence of silica template is not an insurmountable problem. Han's group has also reported the synthesis of mesostructured CuS from CdS via cation exchange, in which the CdS nanoparticles was supported by the surfactant micelles array.¹¹ Both of his and our results proved the high efficiency of cation exchange.

Conclusions

Ordered mesoporous CdS with a complex cubic *Im3d* gyroid 3D bicontinuous porous structure and large particle size was used as precursor for the syntheses of ordered mesoporous Ag₂S and CuS via cation exchange reaction. For CuS, it is found that the mesostructure can be well retained after the chemical transformation, despite of a 21% volume shrinkage occurred during the reaction. The same crystal structure of CdS and CuS is an important issue for this successful cation exchange reaction. While for Ag₂S, the ordered mesostructure is collapsed during the cation exchange reaction unless the mesoporous silica template is present as a matrix support. In addition, the cation exchange reaction is sufficiently enough for a completely composition conversion even when the mesostructured CdS precursor is embedded inside a mesoporous silica matrix. In this case, ordered mesoporous Ag₂S and CuS can both be successfully synthesized. Our results indicate that cation exchange reaction may be applied to highly complex nanostructures with extremely larger particle sizes.

Acknowledgements

This work was supported by the Program for New Century Excellent Talents in University (NCET-12-1083), NSFC (21003035, 21103038), PCSIRT (IRT1231), NSF of Zhejiang Province (Y4100077, LZ13B030001).

Notes and references

^a College of Material, Chemistry and Chemical Engineering, Hangzhou Normal University, Hangzhou, Zhejiang 310036, China.

^b School of Materials Science and Engineering, Wuhan Textile University, Hubei 430200, China.

^c Hangzhou Nanosemi Sci-Tech Co., Ltd., Hangzhou, Zhejiang 310010, China.

Electronic Supplementary Information (ESI) available: XRD patterns and nitrogen sorption data of the KIT-6 template, CdS precursor, Ag₂S and CuS products. See DOI: 10.1039/b000000x/

1. J. C. Lytle, H. W. Yan, R. T. Turgeon and A. Stein, *Chemistry of Materials*, 2004, **16**, 3829-3837.
2. Y. Shi, F. Zhang, Y.-S. Hu, X. Sun, Y. Zhang, H. I. Lee, L. Chen and G. D. Stucky, *Journal of the American Chemical Society*, 2010, **132**, 5552-+.
3. H. Tueysuez, Y. Liu, C. Weidenthaler and F. Schueth, *Journal of the American Chemical Society*, 2008, **130**, 14108-+.
4. Y. F. Shi, Y. Wan and D. Y. Zhao, *Chemical Society Reviews*, 2011, **40**, 3854-3878.
5. P. H. C. Camargo, Y. H. Lee, U. Jeong, Z. Q. Zou and Y. N. Xia, *Langmuir*, 2007, **23**, 2985-2992.
6. D. H. Son, S. M. Hughes, Y. D. Yin and A. P. Alivisatos, *Science*, 2004, **306**, 1009-1012.
7. R. D. Robinson, B. Sadtler, D. O. Demchenko, C. K. Erdonmez, L. W. Wang and A. P. Alivisatos, *Science*, 2007, **317**, 355-358.
8. B. J. Beberwyck, Y. Surendranath and A. P. Alivisatos, *The Journal of Physical Chemistry C*, 2013, **117**, 19759-19770.
9. J. M. Luther, H. M. Zheng, B. Sadtler and A. P. Alivisatos, *Journal of the American Chemical Society*, 2009, **131**, 16851-16857.
10. B. Sadtler, D. O. Demchenko, H. Zheng, S. M. Hughes, M. G. Merkle, U. Dahmen, L. W. Wang and A. P. Alivisatos, *Journal of the American Chemical Society*, 2009, **131**, 5285-5293.
11. C. R. Lubeck, T. Y. J. Han, A. E. Gash, J. H. Satcher and F. M. Doyle, *Advanced Materials*, 2006, **18**, 781-+.
12. Y. Wan and D. Y. Zhao, *Chemical Reviews*, 2007, **107**, 2821-2860.
13. M. G. Kanatzidis, *Advanced Materials*, 2007, **19**, 1165-1181.
14. Y. Shi, C. Hua, B. Li, X. Fang, C. Yao, Y. Zhang, Y.-S. Hu, Z. Wang, L. Chen, D. Zhao and G. D. Stucky, *Advanced Functional Materials*, 2013, **23**, 1832-1838.
15. F. Chen, J. Wang, B. Li, C. Yao, H. Bao and Y. Shi, *Materials Letters*, 2014, **136**, 191-194.
16. B. T. Yonemoto, G. S. Hutchings and F. Jiao, *Journal of the American Chemical Society*, 2014, **136**, 8895-8898.
17. F. Kleitz, S. Hei Choi and R. Ryoo, *Chemical Communications*, 2003, 2136-2137.
18. X. Y. Liu, B. Z. Tian, C. Z. Yu, B. Tu, Z. Liu, O. Terasaki and D. Y. Zhao, *Chem. Lett.*, 2003, **32**, 824-825.
19. R. Thiruvengadathan and O. Regev, *Chem. Mat.*, 2005, **17**, 3281-3287.
20. Y. Ren, Z. Ma and P. G. Bruce, *Chemical Society Reviews*, 2012, **41**, 4909-4927.
21. Y. F. Shi, Y. Wan, R. Y. Zhang and D. Y. Zhao, *Advanced Functional Materials*, 2008, **18**, 2436-2443.
22. D. Routkevitch, T. L. Haslett, L. Ryan, T. Bigioni, C. Douketis and M. Moskovits, *Chemical Physics*, 1996, **210**, 343-352.
23. B. Minceva-Sukarova, M. Najdoski, I. Grozdanov and C. J. Chunnillal, *Journal of Molecular Structure*, 1997, **410-411**, 267-270.
24. I. Martina, R. Wiesinger, D. Jembrih-Simb⁻¹ rger and M. Schreiner, *E-Preservation Science*, 2012.

